Proceedings of the 1991
Coalbed Methane Symposium
The University of Alabama/Tuscaloosa
May 13-16, 1991

9143

The 1991
Coalbed Methane Symposium

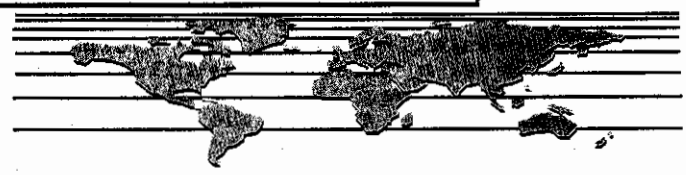

Multiphase Flow In a Fracture

L. J. Pyrak-Nolte (Purdue University)

ABSTRACT

Three approaches are undertaken to study invasion of a wetting phase fluid into a simulated fracture completely saturated by a non-wetting phase. The case of invading methane gas into a brine saturated fracture is examined based only on capillary pressure effects. Fracture void geometries are generated using a stratified continuum percolation model. The fracture void simulations exhibit a lognormal aperture distribution and are spatially correlated. The three approaches used are: (A) ordinary percolation with global accessibility; (B) ordinary percolation with inlet accessibility; and (C) ordinary percolation with inlet accessibility but with trapping. Trapping refers to the trapping of the non-wetting phase by the wetting phase and depends on the spatial correlations of the void spaces in the fracture. For the fracture void simulations used here, the non-wetting phase is trapped in regions of local maxima in the aperture distribution. By including the effects of trapping for multiphase flow through a fracture, a dramatic reduction of relative permeability (six percent of absolute permeability) and a high residual non-wetting phase saturation (sixty percent) are predicted. Fractures under stress are found to have reduced permeabilities and increased residual non-wetting phase saturation.

INTRODUCTION

Understanding how multiphase flow occurs in fractures in rock is of great importance to many area of geophysical research and exploration, such as the recovery of methane from coalbeds, the recovery of oil from fractured reservoirs, nuclear waste isolation, gas storage in underground caverns, and recharge of geothermal systems. Coalbed permeability is primarily controlled by the cleat (fracture) system in the coalbed. The geometry and distribution of cleats in coal depend on the rank of coal and the local stress regime. Often, it is difficult to predict the flow characteristics of coalbeds caused by fractures because changes in local stress or reservoir pressures will open and close fractures affecting the permeability. Also, the permeability of a gas phase and a liquid phase in a fracture will differ depending on the saturation of each phase.

Multiphase flow through a fracture is fundamentally different than multiphase flow through a porous medium. In a fracture, fluid flow occurs in a two-dimensional plane and is determined by the aperture distribution. The complexity of the void space geometry in a fracture arises because a fracture consists of two rough surfaces in partial contact. Between areas of contact, there exist voids of variable aperture and various geometry. The key to understanding multiphase flow through a fracture is to understand how the distribution of each phase depends on the fracture topology and how the fluids are introduced into the fracture.

In reviewing the literature, few experimental measurements have been made of fracture-relative permeability ([1], [2], [3], [4]). These experiments were performed on artificial fractures or fractures represented by parallel glass plates. Several investigators have undertaken theoretical investigations of multiphase flow in fractures. Some models involve the use of capillary theory to study multiphase flow through fractures idealized as parallel plates ([5], [6], [7]) or wedge-shaped fractures with continuously varying apertures [8]. Pruess & Tsang [1] numerically analyzed relative permeabilities of a rough-walled fracture, for a lognormal aperture distribution with various spatial correlations. They found that relative permeabilities are sensitive to the nature and range of spatial correlation of the apertures. Pyrak-Nolte et al, [9] examined unsaturated flow in single fractures for the case of a non-wetting phase was invading a wetting phase fluid (such as mercury injected into a fracture saturated with air in rock).

In this paper, relative permeabilities and capillary pressures are determined for fracture void geometries generated by a stratified continuum percolation model.

These fracture void simulations exhibit the spatial correlations observed in natural fractures. Three approaches are used to invade a wetting phase fluid into a fracture saturated by non-wetting phase: (A) ordinary percolation with global accessibility (similar to that of Pruess of Tsang); (B) ordinary percolation with inlet accessibility; (C) ordinary percolation with inlet accessibility and with trapping. Approach (C) allows the wetting phase fluid to trap the non-wetting phase fluid at local maxima in the aperture distribution. The effect of trapping in the analysis of multiphase flow through fractures results in a high residual non-wetting phase saturation and a very low relative wetting phase permeability.

FRACTURE MODEL

A stratified continuum percolation model ([10], [11]) is used to generate three-dimensional simulations of fracture void geometries to investigate two-phase flow in a fracture. The fracture void simulations from this model exhibit the spatial correlations and aperture distribution observed in natural fractures. The stratified continuum percolation model consists of a correlated skeleton upon which standard random percolation patterns are applied. A continuum model is used because the distribution of void apertures is continuous and there is no underlying lattice structure in a fracture.

A flow path geometry is generated by placing N random sites within a region called a tier. Each of these sites represents the center of a new tier smaller than the preceding tier by a scale factor. In each of the new tiers, N sites that define the center of yet another new series of tiers, which are smaller than the preceding tier by the same scale factor, are again randomly distributed. This process can continue for as many tiers as desired. Within each of the smallest tiers (or the final tiers), N sites are randomly plotted, resulting in a black and white correlated pattern. Figure 1 represents a fracture under low stress because of the small amount of contact area (white regions in Figure 1). This pattern was generated using a five tier model with twelve points per tier and a scale factor of 2.37 between tiers.

As the points are being plotted to construct the pattern, points will overlap. The amount of overlap that occurs at each pixel of the pattern is counted and equated to fracture aperture (arbitrary units). The aperture distribution of the pattern is related to the density of sites in the construction of the pattern. Figure 2 is a contour map of the aperture distribution of the pattern shown in Figure 1. White areas in Figure 2 represent contact areas, and black areas sites of largest apertures. The aperture distribution is correlated because sites of large apertures have a high probability of being surrounded by other sites of large apertures. This model yields a lognormal aperture distribution as observed for many natural fractures ([12], [13]), and yields correlated contact area distributions and aperture distribution.

WETTING PHASE AND NON-WETTING PHASE FLOW PATHS

The flow of two immiscible fluids through a fracture depends on the distribution of the two phases in the fracture void geometry. In this paper, it is assumed that the distribution of each phase depends only on capillary pressure effects (capillary pressure is proportional to the ratio of surface tension of the fluid to the aperture the fluid is occupying) and neglects the effects of viscous and buoyant forces. The term "non-wetting phase" will refer to a fluid that has a high contact angle when in contact with the fracture surfaces and with the other fluid. The term "wetting phase" will refer to a fluid that has a low contact angle when in contact with the fracture surfaces and with the non-wetting fluid.

The configuration of the flowpaths of the wetting and non-wetting phases are based on the local fracture geometry and are independent of global pressure gradients. The assumption is made that the area occupied by each phase is directly dependent on the capillary pressure. The capillary pressure is taken to be inversely proportional to the aperture. When the non-wetting phase is in a small aperture, this corresponds to a high capillary pressure. How the two phases are introduced into the fracture will affect the relationship between capillary pressure and saturation of the fracture. The three approaches (ordinary percolation with (A) global accessibility, (B) inlet accessibility, and (C) inlet accessibility with trapping) are taken to introduce wetting phase fluid into a fracture completely saturated by a non-wetting phase fluid, as discussed below. Wetting phase invasion is equivalent to lowering reservoir pressures on a coalbed reservoir saturated with brine. Cases (A), (B), and (C) will be referred to as global accessibility, inlet accessibility, and inlet accessibility with trapping, respectively, throughout the paper.

(A) Ordinary Percolation with Global Accessibility

Ordinary percolation with global accessibility means that the wetting phase can occupy all sites with aperture b or less even if they are not connected to the inlet. Calculating flow through the fracture simulations begins by initially saturating the fracture with non-wetting phase (meaning the capillary pressure is very high). The wetting phase is introduced into sites with apertures b or less. This corresponds to lowering the capillary pressure. If there is no connected path of wetting phase across the

pattern, then the wetting phase is not flowing and the capillary pressure needs to be lowered again, that is, the value of b increases. This procedures continues until the fracture is completely saturated with wetting phase.

Figure 3 shows the results of global accessibility at breakthrough (when the wetting phase first forms a connected path across the fracture simulation). Notice the disconnected blobs of wetting phase in Figure 3. At the lowest capillary pressure, when the fracture is entirely saturated with wetting phase, the geometry of the wetting phase flow path is the same as that in Figure 1.

(B) Ordinary Percolation with Inlet Accessibility

Ordinary percolation with inlet accessibility means that the wetting phase is invaded from the inlet of the fracture void simulation where sites with aperture b or less are occupied if connected to the invading front. This differs from "invasion" percolation [14] for which the wetting phase occupies the site with smallest aperture along the invading front even if it is not the smallest aperture of the entire pattern.

The inlet accessibility approach begins with the simulated fracture saturated with non-wetting phase (under high capillary pressure). The wetting phase is introduce from the inlet of the fracture simulation by lowering the capillary pressure, that is, by occupying sites along the invading front of aperture b or less. If the sites are not connected to the invading front but have an aperture less than b, these sites remain filled with non-wetting phase. If there is not a connected path of wetting phase across the pattern, then the wetting phase is not flowing and the capillary pressures needs to be lowered again; the value of b increases. This procedure continues until the wetting phase completely saturates the fracture simulation. This approach assumes that the non-wetting phase can always exit the fracture.

Figure 4 shows the effect of inlet accessibility on the wetting phase flow path at breakthrough. Unlike global accessibility, there are no unconnected blobs of wetting phase. At the lowest capillary pressure, when the fracture is entirely saturated with wetting phase, both global accessibility and inlet accessibility result in the wetting phase completely saturating the fracture; the wetting phase flow paths are the same as that in Figure 1.

(C) Ordinary Percolation with Inlet Accessibility & Trapping

Ordinary percolation with inlet accessibility and trapping refers to the approach where wetting phase is introduced from the inlet of the fracture simulation and occupies sites with wetting phase for all sites of aperture b or less connected to the invading front, unless the non-wetting phase occupying the site is completely surrounded by wetting phase. If the non-wetting phase is completely surrounded by the wetting phase, the non-wetting phase is trapped and no longer participates in the flow and those sites can never be occupied by the wetting phase.

The inlet accessibility with trapping approach begins with the fracture completely saturated with non-wetting phase (high capillary pressure). The wetting phase is introduced from the inlet of the fracture simulation by lowering the capillary pressure. A site along the invading wetting phase front is occupied if the site has an aperture of b or less and the site is not completely surrounded by wetting phase. If the site is surrounded, the non-wetting phase is trapped and the wetting phase is not allowed to occupy this site for the rest of the simulation. The capillary pressure is lowered (value of aperture is increased) until the non-wetting phase is disconnected from the exit.

Figures 5 & 6 show the effect of trapping on the geometry and distribution of the wetting phase flow paths when the wetting phase breaks through, and when the non-wetting phase no longer flows. At wetting phase breakthrough, saturation of the wetting phase for inlet accessibility with trapping (approach A, Figure 5) is less than the saturation of the wetting phase for inlet accessibility (approach B, Figure 4). When the non-wetting phase no longer flows, the saturation of the wetting phase cannot be increased because of the effect of trapping (Figure 6). The effect of trapping results in a lower maximum value of wetting phase saturation than that for global accessibility (approach A, Figure 3) or inlet accessibility with no trapping (approach B, Figure 4). Because of the correlated and continuous nature of the void geometry of the simulated fracture, the non-wetting phase becomes trapped in regions of local maxima. Regions of local maxima are surrounded by voids of smaller apertures through which the wetting phase preferentially flows.

CALCULATION OF SATURATION, FLOW AND PERMEABILITY

Five different fracture void simulations were generated from the stratified continuum percolation model, each pattern based on a five-tier construction with twelve points per tier and a scale factor of 2.37 between tiers. Flow was allowed only left to right in the simulations. For each approach and each pattern, volume and area of the wetting phase introduced as a function of aperture were recorded. The percolation threshold of wetting phase and when the non-wetting phase no longer percolated were also noted. The non-wetting phase no longer percolates or flows

when the critical neck for the non-wetting phase is occupied by wetting phase. The critical neck for the non-wetting phase is the smallest aperture along the path of highest apertures (critical path or non-wetting phase critical path) across the pattern. The critical neck for the wetting phase is the largest aperture along the path of smallest apertures across the pattern (wetting phase critical path). In the simulations, it is possible to have both phases flowing or percolating concurrently. Wetting phase saturation is calculated by dividing the volume of wetting phase in the simulated fracture by the total volume of the simulated fracture.

In order to determine the relative permeability of each phase in the simulated fractures, relative flow of each phase through the fracture is evaluated. Relative fluid flow through the fracture is calculated for each increment of capillary pressure (increment of aperture) assuming steady-state equilibrium conditions. In calculating fluid flow through the fracture, a zeroth order approach is taken that includes only the simplest dependences. For determining the wetting phase flow, Q_w, "cubic law" [15] behavior is assumed to describe the local dependence of fluid flow on aperture. The two-dimensional critical behavior is included by a scaling law that describes changes in tortuosity

$$Q_w \propto (b_{eff})^3 (a_w - a_{cw})^t \qquad (1)$$

where b_{eff} is the effective aperture of the wetting phase critical neck, a_w is the area occupied by the wetting phase normalized by the area of the entire simulated fracture, a_{cw} is the normalized area of the wetting phase at threshold, and t is a critical exponent taken to be t=1.9 for these simulations. The critical exponent for standard random continuum percolation ranges between $1.7 < t < 2.7$ [16]. Tortuosity is important for determining the wetting phase flow because the path of the wetting phase is constantly changing with changes in saturation. An effective critical aperture is used for the wetting phase flow evaluation to account for the parallel flow paths that are established as the wetting phase is allowed into larger apertures.

Because the non-wetting phase dominates the critical path of the pattern and only flows along this path, the tortuosity of the non-wetting phase flow path does not change with a change in saturation. The non-wetting phase flow is given by

$$Q_{nw} \propto (b_{cnw})^3 \{1 - (b_w / b_{cnw})\} \qquad (2)$$

where b_{cnw} is the critical neck of the critical path of the fracture simulation, and b_w is the largest aperture the wetting phase has entered for a given capillary pressure. The quantity $\{1 - (b_w / b_{cnw})\}$ in equation (2) represents the change in the width of the non-wetting phase critical neck as the wetting phase is allowed into larger apertures.

Equations (1) and (2) differ slightly from the equations put forth by Pyrak-Nolte et al. [9] to model the displacement of a wetting phase by a non-wetting phase. In [9] the wetting phase flow equation consisted of a sum of cubic law behavior for multiple wetting phase critical necks. In the present paper, the effective aperture gives a better representation of the occurrence of multiple wetting phase flow paths. In [9] the non-wetting flow was assumed to depend on the cube of the non-wetting phase critical neck, and on a linear dependence on the change in area occupied by the non-wetting phase. In the present paper, the non-wetting phase flow equation is based strictly on the effects at the critical neck, that is, the change in the width of the non-wetting phase in the critical neck as the wetting phase invades the small apertures around the critical neck. Which ansatz is a better approximation is beyond the scope of this paper, and is an area of future work.

Relative permeability of each phase in the fracture void simulations were determined from relative flow values ($k_w/k_{tot} \propto Q_w/Q_{tot}$, where k_w is the permeability of the wetting phase, and k_{tot} is the single phase permeability). Flow for each phase was normalized by the flow through the simulation for a hundred percent saturation by the wetting phase ($Qtot \propto (b_c)^3$). The global pressure gradient was assumed equal for both phases. Viscosities are based on the values for methane (108.7 x 10-6 poise) and water (0.01 poise).

RESULTS

Capillary pressure curves for global accessibility, inlet accessibility, and inlet accessibility with trapping are shown in Figure 7 as a function of wetting phase saturation. The capillary pressure curve for a log-normal aperture distribution in a fracture is similar to the customary j function for three-dimensional porous media [1]. The important feature of Figure 7 is the difference between the results for inlet accessibility with trapping and the other two approaches. Trapping of the non-wetting phase by the wetting phase has a dramatic effect on the capillary pressure curves for a single fracture. Because of trapping, lowering the capillary pressure will never result in hundred percent wetting phase saturation. For the simulations, at the lowest capillary pressure, the maximum wetting phase saturation is roughly thirty-five percent.

The effect of stress on the capillary pressure-wetting phase saturation relationship was examined. Stress on the fracture was simulated by reducing the apertures of the simulated fracture geometry. The application of stress results in an increase in contact area, a decrease in void volume and a reduction in

aperture. The apertures in the pattern were reduced by 10 units and 20 units. Figure 8 compares the effect of stress on the wetting phase saturation determined from the inlet accessibility with trapping for 0, 10 and 20 units of aperture reduction with the results of global accessibility at zero stress for reference. The effect of stress is to lower the value of the maximum possible wetting phase saturation. As the apertures are reduced by 10 units, the maximum wetting phase saturation is reduced from thirty-five percent to twenty-six percent. A reduction of aperture by 20 units results in a maximum wetting phase saturation of only sixteen percent volume saturation.

The relative permeabilities of each phase as a function of wetting phase saturation are shown in Figure 9 for the three approaches for non-wetting phase fluid displacement by a wetting phase fluid. For wetting phase permeability, the effect of trapping results in a maximum permeability around six percent for a maximum wetting phase saturation of around thirty-five percent. The wetting phase relative permeability for both global accessibility and inlet accessibility reaches a maximum value of one hundred percent for a hundred percent wetting phase saturation.

For non-wetting phase relative permeability, the effect of trapping lowers the value of the non-wetting phase relative permeability with respect to the global access and inlet access approaches. For all three approaches, there occurs a rapid decrease in non-wetting phase permeability with increasing wetting phase saturation.

The cross-over in relative permeabilities represents the value of saturation for which the relative permeabilities of the two phases are equal. The cross-over in relative permeability differs for the three approaches used to invade a wetting phase into a fracture filled with non-wetting phase. For global accessibility the relative permeabilities cross-over at thirty-two percent saturation, while for inlet access with trapping the cross-over occurs at twenty percent wetting phase saturation.

Figure 10 shows the effect of stress (aperture reductions of 10 and 20 units) on the relative permeabilities for the case of inlet accessibility with trapping. Stress on a fracture will lower the relative permeabilities, decrease the maximum wetting phase saturation value, and lower the wetting phase saturation value at which the cross-over in relative permeability of the fracture.

CONCLUSIONS

It is observed that including the effect of trapping of a non-wetting phase fluid by a wetting phase fluid greatly influences the relative permeabilities of each phase for a fracture, the capillary pressure-wetting phase saturation relationship, and also the relative fluid flow through the fracture. For the flow of methane in a cleat saturated with brine, trapping would represent the trapping of brine by methane because of the blockage of flow paths by the methane. Trapping of the brine by methane reduces the percent saturation possible for the methane, and reduces the flow of methane through the fracture. For the simulated fractures, the maximum methane relative permeability for a fracture would be six percent for a maximum saturation of thirty-five percent. The results show that even if capillary pressures were reduced, there would not be an increase in the production of methane from a fracture. Cramer [17] noted that the relative permeability of gas in a coalbed methane reservoir is about ten percent of absolute permeability and that coals have a high residual water saturation. The effect of trapping of brine by methane in fractures may be one explanation for the observed low value of gas relative permeability. Finally, if the fracture is stressed, the methane relative permeability would be further reduced and would result in a high residual brine saturation. These conclusions are based on a fracture aperture distribution that is log-normal. It must still be determined is whether fractures in coal have lognormal aperture distributions, or have other geometric properties which will affect the flow.

ACKNOWLEDGEMENTS

The work reported here was supported by the Gas Research Institute, Contract No. 5090-260-2003 and by Purdue University.

REFERENCES

1. Pruess, K., and Tsang, Y.V., 1990, "On two-phase relative permeability and capillary pressure of rough-walled rock fractures"; Water Resources Research, v. 26, no 9 (September), p.1915-1926.
2. Barton, N.R., 1972, "A model study of air transport from underground openings situated below groundwater level", Proceedings, Symposium International Society for Rock Mechanics, Suttgart, Deutsche Gesellschaft für Erd-und Grundbau, p.T3-A1-T3-A20.
3. Merrill, L.S., Jr., 1975, Two-phase flow in fractures, PH.D. thesis, Univ. of Denver, Denver, Colo..
4. Bawden, W.F., and Rogiers, J.C., 1985, "Gas escape from underground mined storage facilities - A multiphase flow phenomena", in Proceedings, International Symposium on Fundamentals of Rock Joints, Björkliden, edited by O. Stephansson, Center Publishers, Norway, p.503-514.
5. Evans, D.D., 1983, "Unsaturated flow and transport through fractured rock - related to high-level waste repositories", Final Report-Phase I, Dept. Hydrology and Water Resources, University of Arizona, prepared for

U.S. Nuclear Reg. Comm., Report NUREG/CR-3206.
6. Evans, D.D., and Huang, C.H., 1983, "Role of desaturation on transport through fractured rock", in Role of Unsaturated Zone in Radioactive and Hazardous Waste Disposal, eds. J.W. Mercer, P.S.C. Rao, and I.. Marine, Ann Arbor Science, pp. 165-178.
7. Rasmussen, T.C., Huang, C.H., and Evans, D.D., 1985, "Numerical experiments on artificially generated, three-dimensional fracture networks: an examination of scale and aggregation effects", in Mem. Int. Assoc. Hydrogeol., XVII, p.676-682.
8. Rasmussen, T.C., 1987, "Computer simulation model of steady fluid flow and solute transport through three-dimensional fracture networks of variably saturated discrete fractures:, in (eds) Evans and Nicholson, Flow and Transport through Unsaturated Fractured Rock, Geophysical Monograph 42, American Geophysical Union, pp 107-114.
9. Pyrak-Nolte, L.J., Nolte, D.D., Myer, L.R., and Cook, N.G.W., 1990, "Fluid flow through single fractures", in Rock Joints, eds. N. Barton and O. Stephansson, Rotterdam, A.A. Balkema, p. 405-412.
10. Pyrak-Nolte, L.J., Cook, N.G.W., and Nolte, D.D., 1988, "Fluid percolation through single fractures", Geophysical Research Letters, v. 15, no. 11, p1247-1250.
11. Nolte, D.D., 1989, Invariant fixed point in stratified continuum percolation: Physical Review A, v.40, p4817.
12. Gale, J.E., 1987, "Comparison of coupled fracture deformation and fluid flow models with direct measurements of fracture pore structure and stress-flow properties", in Rock Mechanics: Proceedings of the 28th U.S. Symposium, eds Farmer, Daemen, Desai, Glass & Nueman, Rotterdam, A.A. Balkema, p.1213-1222.
13 Hakami, E., 1988, Water flow in single rock joints, Sweden [Ph.D. thesis], Lulea University of Technology, Sweden, p. 99.
14. Wilkinson, D. and Willemsen, J.F., 1983, "Invasion percolation: a new form of percolation theory", J. Phys. A: Math. Gen., vol. 16, p.3365-3376.
15. Witherspoon, P.A., Wang, J.S.Y., Iwai, K., and Gale, J.E., 1980, "Validity of cubic law for fluid flow in a deformable rock fracture", Water Resources Research, v. 16, n. 6, p. 1016-1024.
16. Halperin, B.I., Feng, S., and Sen, P.N., 1985, "Differences between lattice and continuum percolation transport exponents", Phys. Rev. Lett., vol. 54, p.2391.
17. Cramer, D.D., 1989, "Fracturing key element in Fruitland methane activity", Oil and Gas Journal, (October 9), p57-61.

Figure 1. Stratified continuum percolation model of flow paths (black regions) in a fracture for five tiers, twelve points per tier, and a scale factor of 2.37. White regions represent areas of contact.

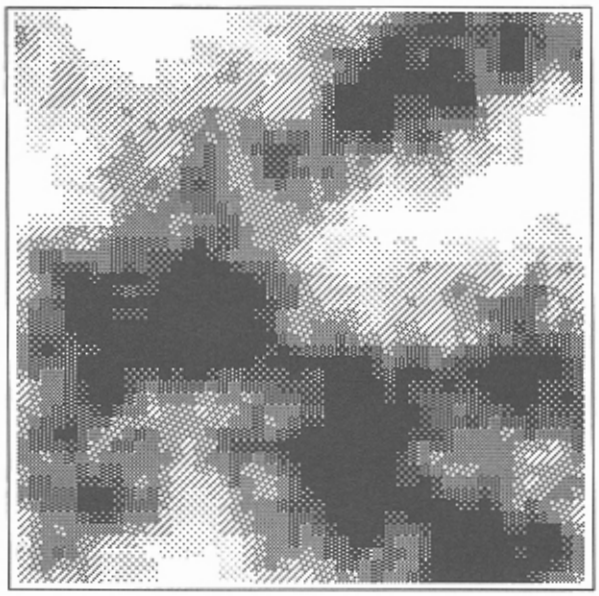

Figure 2. Aperture contour map of pattern in Figure 1. White regions represent contact areas and increasing shades of gray to black represent increasing apertures. The contour interval is 20 units of aperture.

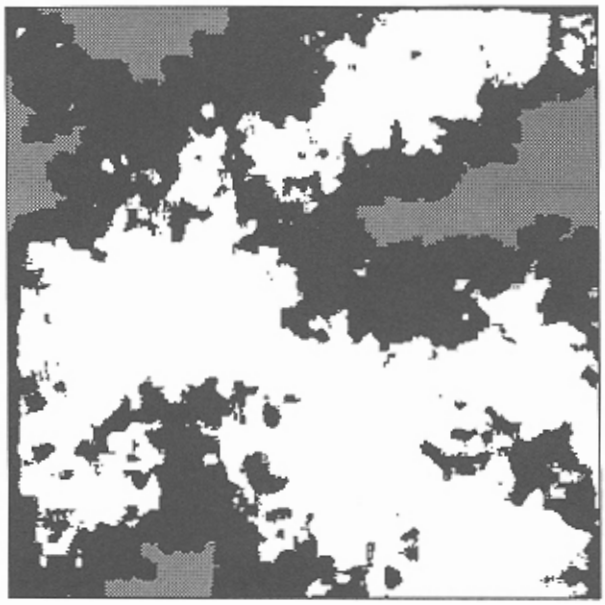

Figure 3. Wetting phase (black regions) flow paths in a fracture for global accessibility. White regions represent non-wetting phase flow paths, and gray regions represent areas of contact. Note unconnected blobs of wetting phase.

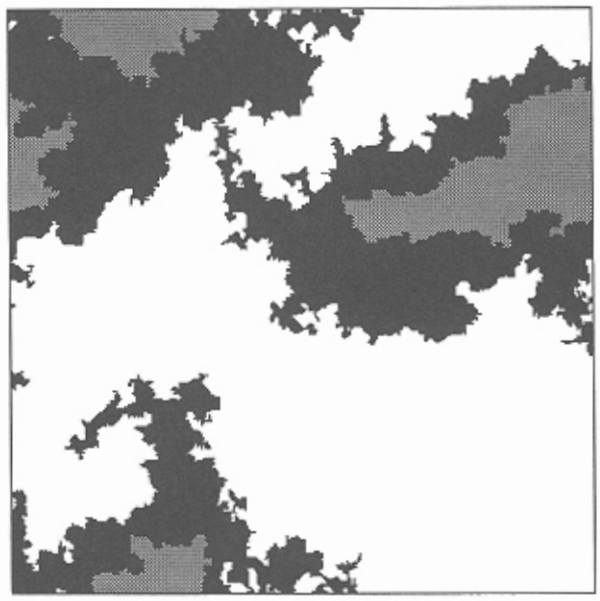

Figure 4. Wetting phase (black areas) flow paths at breakthrough for inlet accessibility. Gray regions represent contact area, and white regions represent the non-wetting phase flow paths.

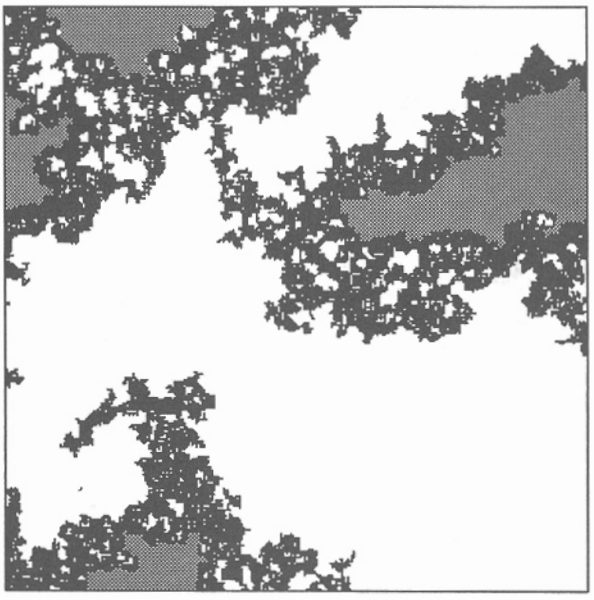

Figure 5. Wetting phase (black regions) flow paths at breakthrough for a fracture with inlet accessibility with trapping. White regions represent the non-wetting phase and gray regions represent contact area. Note the trapped areas of non-wetting phase in the wetting phase flow paths.

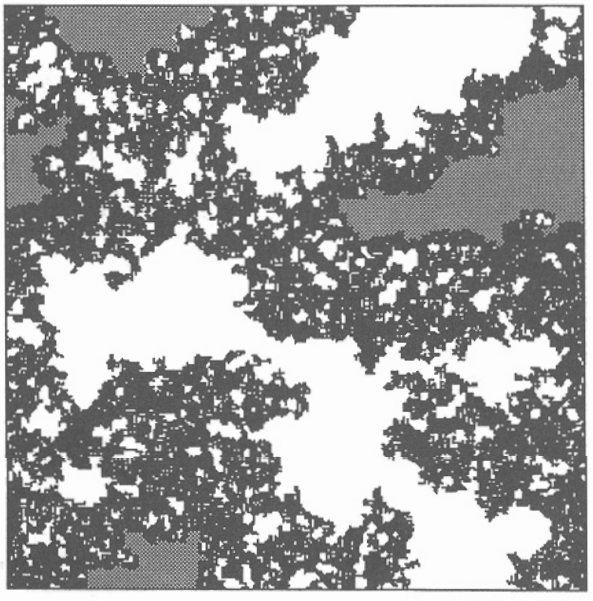

Figure 6. Wetting phase (black regions) flow paths for a fracture when the non-wetting phase (white) no longer percolates for inlet accessibility with trapping. Gray regions represent contact area.

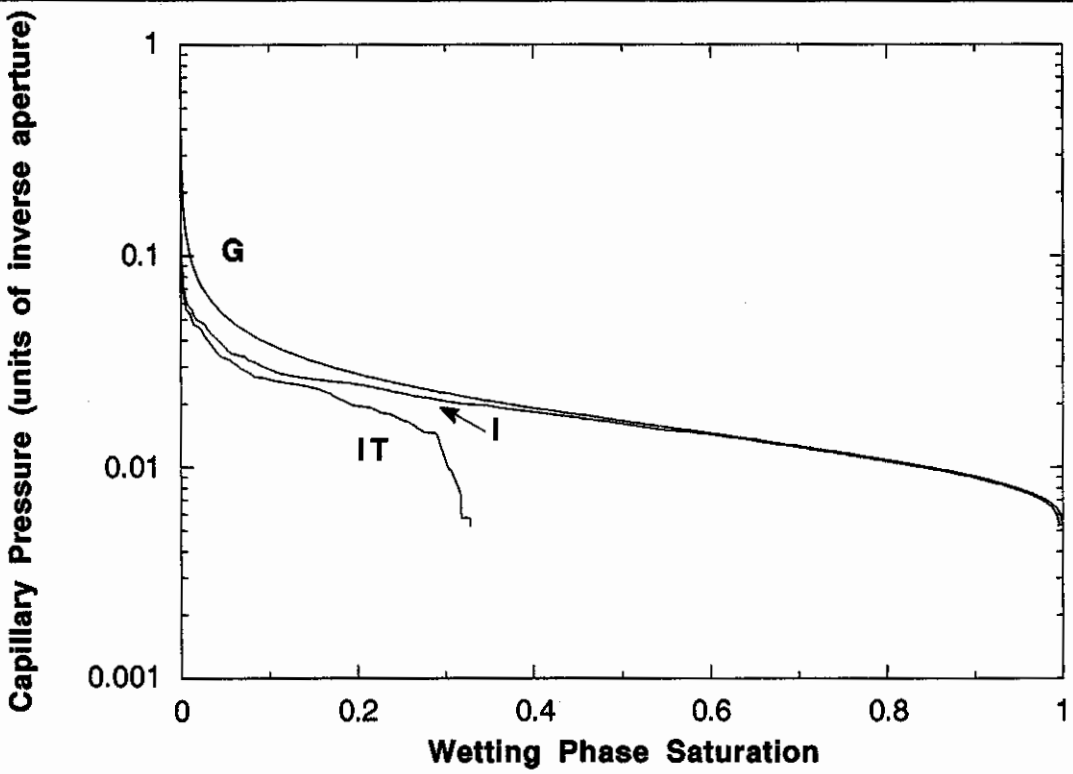

Figure 7. Capillary pressure (inverse aperture) versus wetting phase saturation for a fracture for G - global accessibility; I - inlet accessibility; and IT - inlet accessibility with trapping.

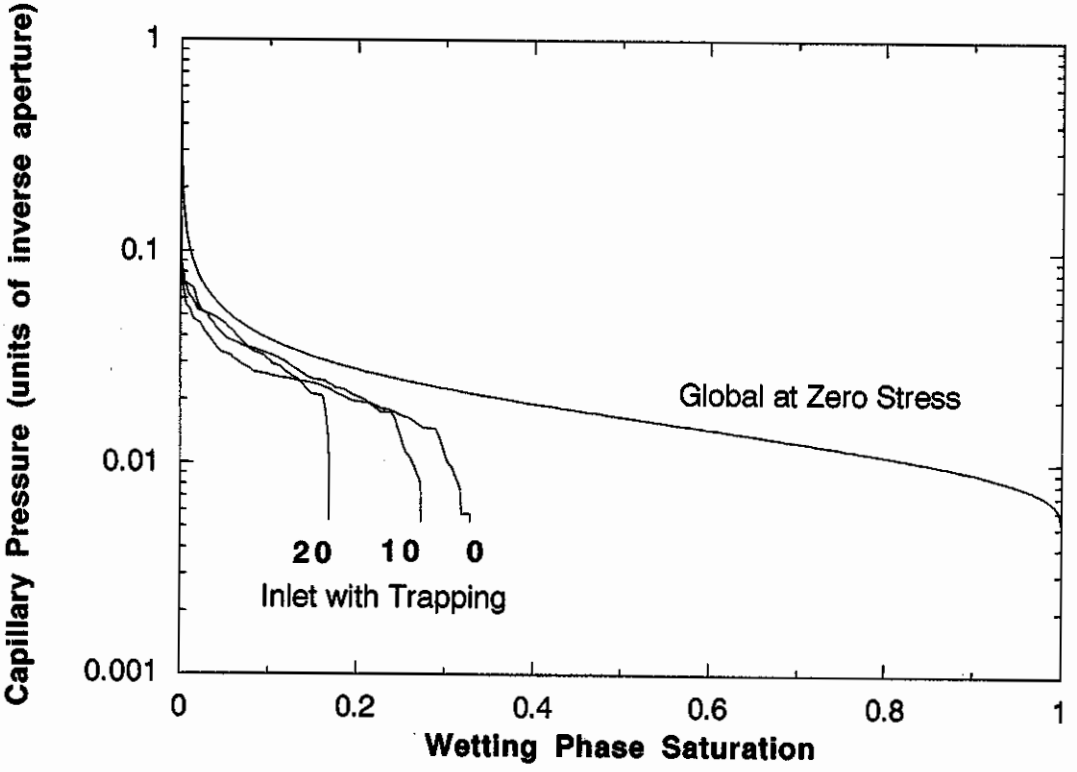

Figure 8. The effect of stress on capillary pressure for inlet accessibility with trapping (for stresses of 0, 10, and 20 units). Results for global accessibility at zero stress are shown for reference.

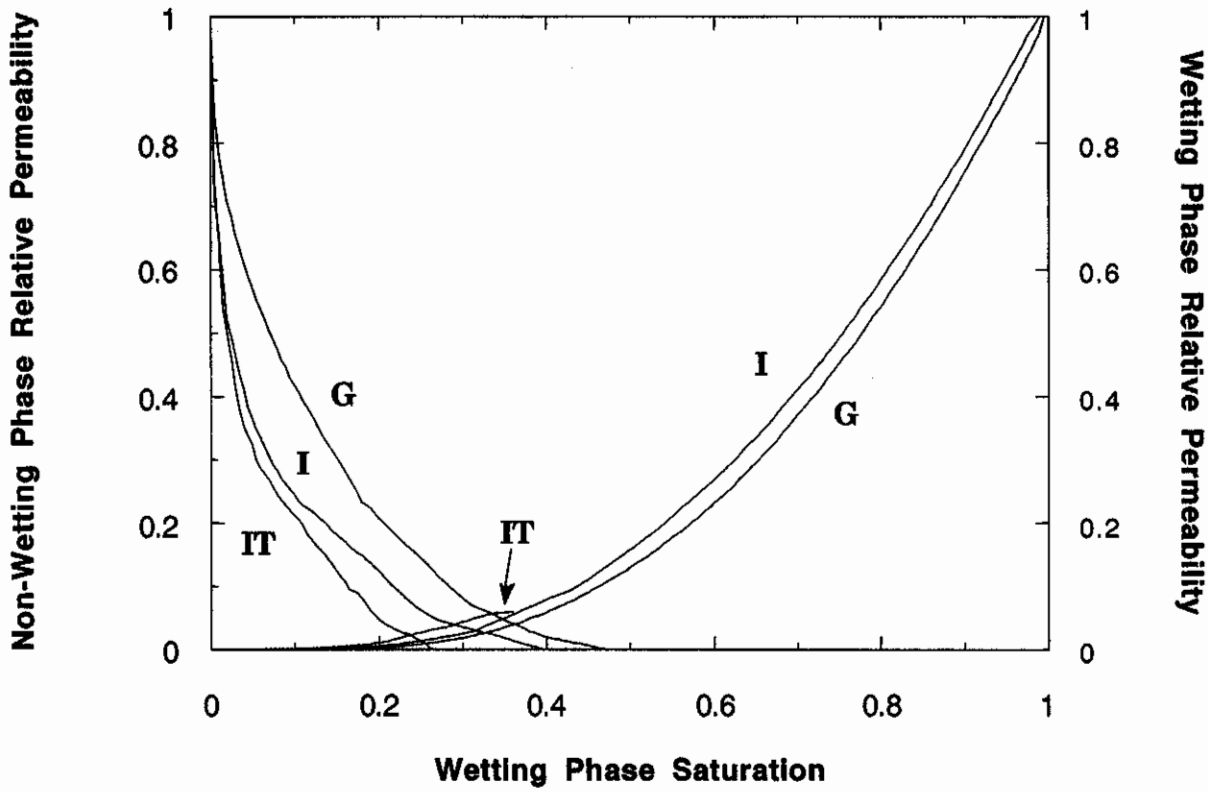

Figure 9. Comparison of relative permeability values for G - global accessibility; I inlet accessibility; and IT - inlet accessibility with trapping for a fracture.

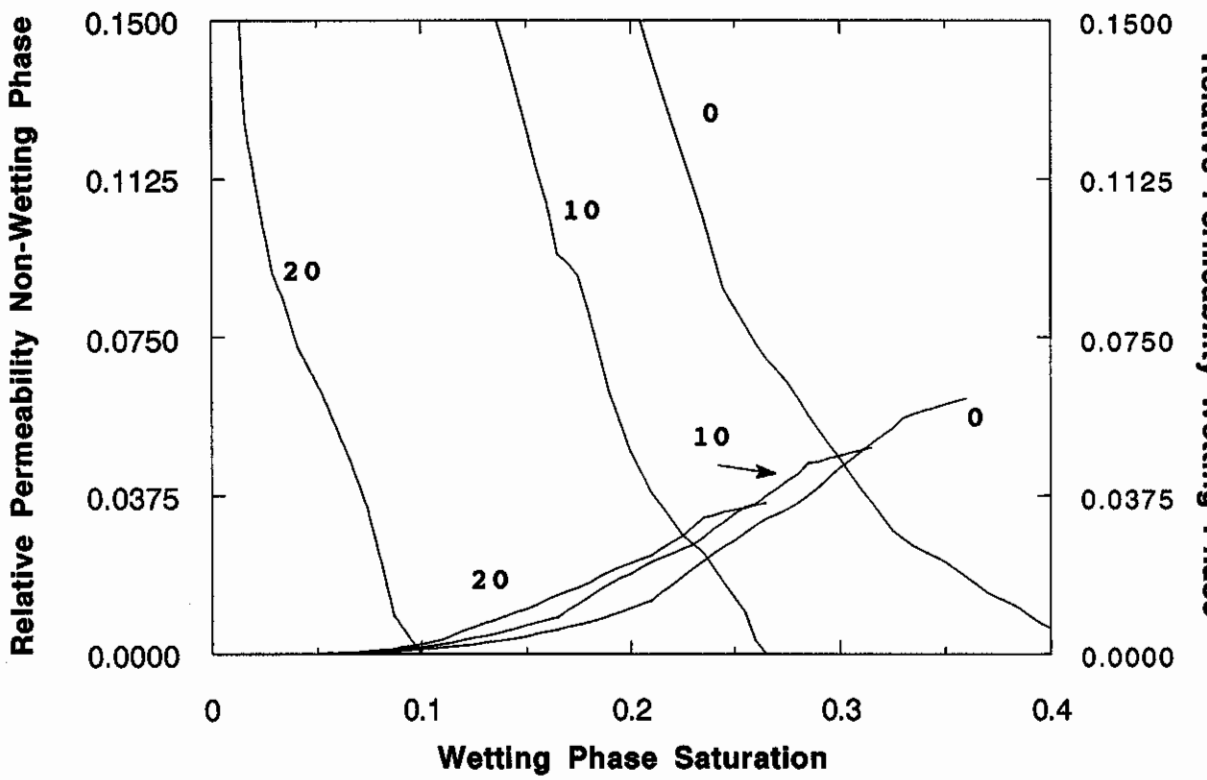

Figure 10. Effect of stress on relative permeability of a fracture with inlet accessibility with trapping for a fracture subjected to stresses of 0, 10 and 20 units.